Indian Journal of Chemistry
Vol. 64, June 2025, pp. 614-618
DOI: 10.56042/ijc.v64i6.16044

Synthesis, characterization and biological activity of Zn, Co, Ni, Mn and Cu complexes with (*E*)-3-(1-(2-(4,6-dimethylpyrimidin-2-yl)hydrazone)ethyl-2-hydroxy-6-methyl-4*H*-pyran-4-one

Suryasri Erukala, Polepaka Anusha Rechel & Sunkari Jyothi*
Department of Chemistry, Kakatiya University, Vidyaranyapuri, Hanamkonda, Warangal 506 009, Telangana, India
E-mail:suryasrimykala@gmail.com

Received 27 November 2024; accepted (revised) 22 May 2025

The DHA derivatives of heterocyclic ring system has potent anti-microbial, anti-fungal, anti-bacterial and anti-cancer characteristics in addition to significant chelating characteristics with several metal ions. The current study involves the synthesis of Schiff base metal complexes using the pyrimidine heterocyclic system and dehydroacetic acid (DHA) with ions of Co^{2+}, Ni^{2+}, Cu^{2}+, Mn^{2+} and Zn^{2+}. The hydrazone ligand is coordinated with the metal complexes of Co^{2+}, Ni^{2+}, Cu^{2+}, Mn^{2+} and Zn^{2+} ions, as determined from the ^{1}H NMR, Mass, UV and FT-IR spectra, *via* O and N donor atoms with deprotonation of the -OH functional group. The ligand-to-metal complexes ratio has been found to be 2:1 using mass spectral data. This article describes the HOMO and LUMO orbitals of their energies. Synthesized metal complexes of Cu^{2+} and Zn^{2+} are shown to have remarkable antibacterial activity. All of the various metal complexes exhibit greater antibacterial activity when compared to free hydrazone.

Keywords: DHA, Pyrimidine, Hydrazone, DFT studies, Anti-bacterial activity

Schiff bases are of highest significance among nitrogen-containing synthetic substances because they have a higher ability to favourably interact with transition metals to create coordination complexes[1]. One of the most prevalent methods for preparing Schiff base is the condensation reaction of primary amine with a carbonyl molecule (aldehyde/ketone)[2]. Schiff base ligand and transition metal ions incorporate to form distinctive coordinate compounds[3]. These compounds are not only visually appealing much like an array of colours, but they also have various potential biological and catalytic capabilities[4].

A metal complex of copper is utilized as a catalyst (Wilkinson's catalyst) in the hydrogenation of olefins[5]. Schiff's bases are useful in medicinal chemistry, biological mechanisms, analytical chemistry, organic and inorganic chemistry due to their propensity to compound with various metals[6-10]. The inclusion of the azomethine group (-C=N-) in Schiff base enhances its reliability in medicinal chemistry[11]. This is due to the presence of two electrons on the -N atom, which actively engage in chelation with transition metal ions[12] (Fig. 1). Schiff base compounds are recognized for their antibacterial, antitumor, anti-fungal, anti-cancer, anti-helminthic, anti-tuberculosis, DNA photo-cleavage, DNA binding, analgesic, antioxidant and anti-viral effects[13-20].

Result and Discussion

In a clean, dry round-bottom flask, pyrimidine hydrazone was dissolved in 70% aqueous EtOH solution while being constantly stirred with a magnetic stirrer. Then, a hot EtOH solution of dehydroacetic acid (DHA) was added gradually. For

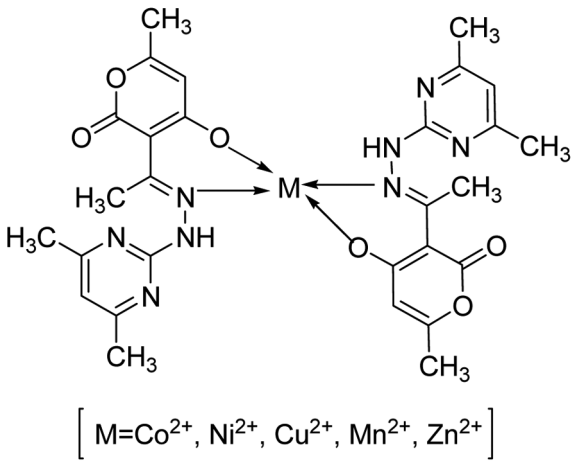

Fig. 1 — Structure of metal complex

three hours, the effect reaction mass was refluxed in a water bath at 75°C. The product has a melting point of 181°C and it is yellowish solid with an 80% yield.

The round-bottomed flask was filled with 0.1 mole of hydrazone ligand and then with MeOH. The first transition series metal acetate was dissolved in 15 cm^3 of MeOH and then added drop-wise to the heated reaction mass. A stoichiometry of 2:1 between the hydrozone ligand and metal was achieved by reflux-heating the reaction mass for 3 h (Scheme 1).

DFT calculations

The B3LYP/6-31G(d,p) approach was used to do all density-functional theory (DFT) computations within the Gaussian 09 software package. In order to accommodate for solvent effects, the optimized geometries (Fig. 2) in solution were calculated using the self-consistent reaction field (SCRF) approach.

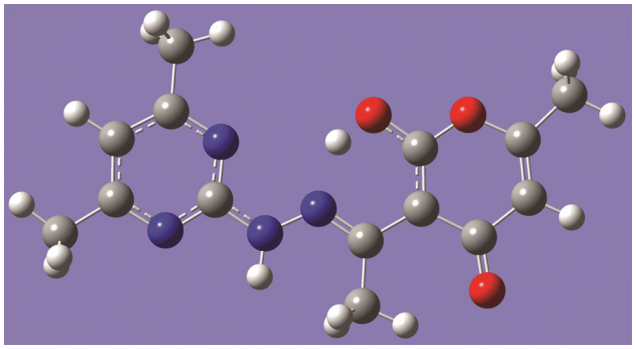

Fig. 2 — Optimised geometry of ligand

Fig. 3 illustrates the presentation of HOMO and LUMO and their respective energies. The presence of both MOs throughout the delocalized π-system suggests an excitation type of π-π* with an energy gap of 3.948 eV, which is the HOMO → LUMO transition. The determined reactivity indices for ionization potential ($I = -E_{HOMO}$), electron affinity ($A = -E_{LUMO}$), chemical potential ($\mu = -(I + A)/2$), hardness ($\eta = (I - A)/2$) and electronophilicity index ($\omega = \mu 2/2\eta$) were –0.244, –0.212, –0.054 and –0.043 eV respectively, according to the HOMO and LUMO energies[21].

Anti-bacterial Study

The technique of well diffusion was used to assess the antibacterial activity of the extracts. A solution of the material in DMSO (1 mg/mL) was prepared for the sample. The medium was then examined for its antibacterial properties.

The antibacterial activity of synthesized Schiff's base hydrazone and its complexes with Co^{2+}, Ni^{2+}, Cu^{2+}, Mn^{2+} and Zn^{2+} ions was tested against bacterial strains such as *Bacillus subtilis, Staphylococcus aureus* and *Pseudomonas syringae, Pseudomonas aeruginosa* using the agar well diffusion method in the presence of DMSO /DMF as a solvent (Table 1). In order to compare the antibacterial activity of synthetic compounds, oxacillin has been chosen as a standard reference medication. The metal complexes demonstrated moderate to exceptional antibacterial activity compared to the ligand under the same experimental circumstances at RT, according to the results. Coordination has been demonstrated to significantly enhance activity. It was determined that the ligand's and its complexes biological effects were

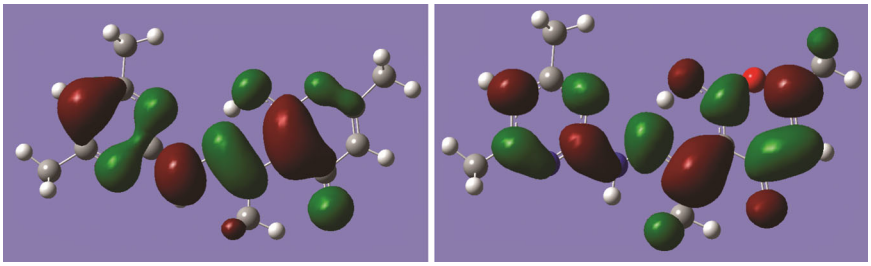

Fig. 3 — The HOMO, LUMO orbitals of the ligand with energies of –0.212 and –0.054

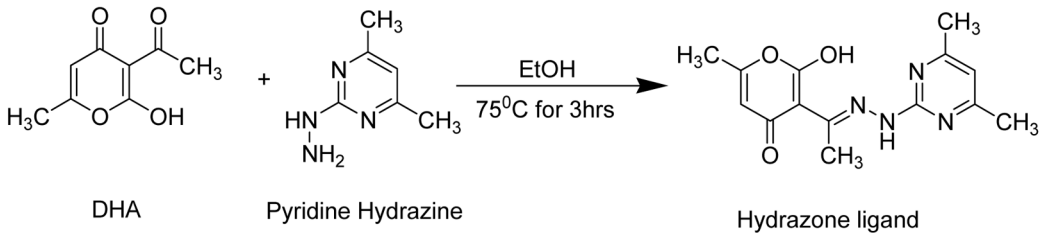

Scheme 1 — Synthetic path way to hydrazone ligand

Table 1 — Anti-bacterial activity data of ligand and its complexes

Compd	Area of Inhibition (mm)			
	B. subtilis	*S. aureus*	*P. syringae*	*P. aeruginosa*
Ligand	8	8	8	8
Co(II)	12	8	14	8
Ni(II)	14	26	15	14
Cu(II)	28	31	26	24
Mn(II)	10	13	8	10
Zn(II)	10	27	22	22
Oxacillin	38	33	37	33

Table 2 — Physical data of ligand and metal complexes

Compd	Color	m.p. (°C)	Elemental analysis – Found			
			C	H	N	M
Ligand	Light yellow	181	58.32	5.59	19.43	–
Co(II)	Light orange	275-277	53.08	4.77	17.69	9.30
Ni(II)	Dark grey	>280	53.10	4.77	17.69	9.27
Cu(II)	Light green	>280	52.70	4.74	17.56	9.96
Mn(II)	Pale yellow	255-257	53.42	4.80	17.80	8.73
Zn(II)	White	253-255	52.55	4.72	17.51	10.22

categorized as Order. The increased ligand Cu activity is demonstrated by the fact that, upon connecting with metal ions, the polarity of Cu^{2+} ions decreases more considerably due to ligand orbital overlap and a partial distribution of the metal ion's positive charge with donor groups.

Experimental Section

To determine the structure of the produced molecules, a variety of approaches were used. The Avance-(II) Bruker 400 model was used to record the ^{1}H and ^{13}C NMR of hydrazone and their metal complexes at 100 and 400 megahertz, respectively, using tetramethylsilane as a reference standard. All of the produced compounds underwent CHN analysis using a Perkin Elmer 2400 CHN elemental analyzer. Using the KBr pellets approach, the Perkin Elmer-spectrum RX-1 FT-IR model was used to investigate the infrared spectra of hydrazone and its complexes. Mass spectra were recorded using the Agilent Mass Spectrometer. Using dimethyl sulfoxide as a solvent and a Shimadzu UV 1800 analyzer, the electronic spectra of the produced compounds were examined. All the chemicals was acquired from Merck and used without distillation. All DFT calculations were performed using Gaussian 09 software package utilizing the B3LYP/6-31G(d,p) method.

Synthesis of Ligand

Pyrimidine hydrazine (0.05 mol) was dissolved in 40 cm^3 70% aqueous EtOH solution with continuous stirring on a magnetic stirrer in a clean and dry 100 cm^3 round bottom flask, followed by the gradual addition of 30 cm^3 hot EtOH solution of dehydroacetic acid (DHA) (0.05 mol). The consequence reaction mass was refluxed in a water bath for 3.0 hours at 75°C. TLC was used to visualize the improvement of the reaction. When the reaction was done, it was cooled to RT. The yellowish crystals obtained were filtered and carefully washed with an excessive amount of cold EtOH. It was crystallized from EtOH and dried in a vacuum air dryer to eliminate any solvent residue. Product is yellowish solid with an 80% yield and a melting point of 181°C.

Synthesis of Metal complexes

In a 100 cm^3 round bottom flask, 0.1 mole of hydrazone ligand was added, followed by 50 cm^3 of MeOH. To obtain a clear solution, the temperature was raised to 75-80°C and stirred continuously for 15 minutes. After dissolving metal acetate (0.1 or 0.05 mole) of the first transition series in 15 cm^3 MeOH, it was added drop-wise to the reaction mass that had been heated above. For three hours, the reaction mass was heated to reflux in order to create complexes that were 2:1 Hydrazone ligand to metal stoichiometric. The solid precipitate of metal complexes was filtered and washed with cooled MeOH, followed by two washes with a non-polar solvent to remove any impurities. Metal complexes were kept in an oven at 50-55°C for 3-4 hours to eliminate solvent residues. All produced compounds were coloured except for the Zn(II) complex (Table 2).

Table 3 — FT-IR data of ligand and its complexes

Compd	IR Frequency (Stretching in cm^{-1})					
	υOH	υC=N	υC=O	υC-O	υM-N	υM-O
Ligand	3445	1575	1682	1001	–	–
Co(II)	3444	1522	1676	1005	648	530
Ni(II)	3430	1523	1677	1007	649	530
Cu(II)	3394	1540	1654	1014	641	531
Mn(II)	3447	1524	1686	1002	646	531
Zn(II)	3444	1525	1388	1002	648	532

Infrared Spectra

A flexible method for examining the binding mechanism and determining which hydrazine donor atoms performed responsibility for coordination with metal ions is infrared spectroscopy. To determine the binding mode, the infrared spectra of ligand was compared to that of synthetic metal complexes. The resulting distinctive IR stretching frequencies are displayed in Table 3. In ligand , IR stretching frequencies were observed at 3445, 1575,1682 and 1001 cm^{-1}. These frequencies may be attributed to υ OH (intramolecular hydrogen bonding), υ C=N (azomethine str.), υ C=O (carbonyl str.) and υ C-O (enolic str.), respectively. In the case of metal complexes, all of the stretching frequencies previously stated were likewise noted, although with some positional movement. The participation of this azomethine N atom of hydrazine in cooperation with metal ions was suggested by the downward change in stretching frequencies caused by υ C=N in the case of a metal complex. Additionally, when comparing the stretching frequencies of υ C=O in metal complexes to ligand, there is no apparent shift, indicating that the carbonyl -O atom does not participate in coordination with metal ions.

The involvement of the –O donor atom of ligand in cooperation with metal ions was suggested by the observed upward shift in υC-O stretching frequencies in the case of metal complexes. Due to υ M-N and υ M-O, which demonstrated the coordination of hydrazone with metal ions *via* oxygen and nitrogen donor atoms of ligand, two additional stretching frequencies were provided in the range of 588-649 and 473-534 cm^{-1} in the case of metal complexes. This further supported the involvement of N and O atoms in coordination as well as the creation of metal complexes. The presence of water molecule traces may be the cause of the band around 3400–3500 cm^{-1} in the infrared spectrum data.

Table 4 — UV-VIS spectrum data of ligand and its complexes

Compd	λ_{Max} (nm)
Ligand	352.02, 275.34, 237.98
Co(II)	363.58, 301.98, 261.90
Ni(II)	343.41, 266.92
Cu(II)	387.07, 305.37
Mn(II)	340.47, 280.97
Zn(II)	345.65, 280.96

Mass Spectra

The ligand and its transition metal complexes with cobalt (II), nickel (II), copper (II), zinc (II) and manganese(II) are displayed together with their mass fragmentation spectral data. Mass spectrometry was used to confirm the mass of ligand and its compounds. The molecule [M+1] ion peak was located at *m/z* = 288.2 in the mass spectra of ligand. The molecular peaks for the Co(II), Ni(II), Cu(II), Mn(II) and Zn(II) complexes were found at *m/z* 633.3[M+1], 632[M+1], 637.2[M+1], 629.1[M+1] and *m/z* 638.1[M+1] in that sequence.

UV-Visible Spectra

As demonstrated in the Table 4, the UV-VIS spectra of ligand and all of its produced metal complexes revealed that methyl sulfoxide had a molar concentration of 10^{-4}.Four bands were seen in the UV spectra at 352.02 nm, 275.34 nm and 237.98 nm at Schiff's base (ligand). The intra ligand π-π* and n-π* transition of >C=O or -C=N group in hydrazine is responsible for these absorption bands. In the case of all produced metal complexes, these bands moved to higher frequencies with hypsochromic shift, indicating that the nitrogen of the -C=N group was involved with the metal ions.

NMR Spectra

Ligand and its metal complex with transition metals were analyzed by ^{1}H and ^{13}C NMR in deuterated dimethyl sulfoxide (DMSO-d_6) using tetra-methylsilane as a reference standard. Every NMR

spectrum was included in the accompanying documentation. The ligand NMR spectra and its metal complexes are shown. The signal at δ 2.60 (singlet, 3H) was caused by -CH_3 of -N=C-CH_3, δ 2.12 (singlet, 3H) by -CH_3 of DHA, δ 5.83 (singlet, 1H) by DHA ring proton, δ 6.90 (singlet, 1H) and δ 8.50 (doublet, 2H) by pyrimidine ring proton, δ 16.53 (broad singlet, 1H) due to -OH proton, and δ 10.68 (singlet, 1H) due to -NH proton, were all detected by the ^{1}H NMR of ligand.

Similarly, The ^{1}H NMR of spectra of Zn complex showed thesignal at δ 2.09 (singlet, 3H) due to -CH_3 of -N=C-CH_3, δ 2.38 (singlet, 3H) due to -CH_3 of DHA, δ 5.74 (singlet, 1H) due to DHA ring proton, δ 6.89 (singlet, 1H), δ 8.30 (singlet, 1H) and δ 8.60 (singlet, 1H) due to pyrimidine ring proton, δ 11.10 (singlet, 1H) due to -NH proton and δ 1.77 (singlet, 3H) due to –CH_3 of -CH3COO.

Conclusion

The accomplished metal complexes of Co^{2+}, Ni^{2+}, Cu^{2+}, Mn^{2+} and Zn^{2+} ions interact with ligand *via* O and N donor atoms with deprotonation of -OH functional group, according to the ^{1}H NMR, Mass, UV and FT-IR spectrum data. The metal salts to ligand stoichiometry was determined to be 1:2 based on mass spectrum data. Cu^{2+} and Zn^{2+} metal complexes that were synthesized were discovered to have outstanding antibacterial activity. When compared to free hydrazone, all other metal complexes had strong antibacterial activity.

Supplementary Information

Supplementary information is available in the website http://nopr.niscpr.res.in/handle/123456789/58776.

Acknowledgements

The authors are grateful to the Director of the Indian Institute of Chemical Technology in Hyderabad. Kakatiya University's Principal, Hanumakonda. Director of the Center for Cellular and Molecular Biology, Hyderabad. Because of the spectral data and biological significance they provide.

Conflict of Interest

The authors have confirmed that there is no conflict of interest.

References

1 Raman N & Selvan A, *Russion J Inorg Chem*, 56 (2011) 759.
2 Abdallah S M, Zayed M A & Mohamed G G, *Arab J Chem,* 3 (2010) 103.
3 Sari N, Gurkan P, Cete S & Sakiyan I, *Russion J Coord Chem,* 32 (2006) 511.
4 Ginley J M, Cann M M, Ni K, Tallon T, Kavanagh K, Devereux M, Ma X & Kee V M, *Polyhedron,* 55 (2013) 169.
5 Patil M, Hunoor R & Gudasi K, *Eur J Med Chem*, 4 (2010) 2981.
6 Emara A A, Ali A M, Ragab E M & Asmy A A E, *J Coord Chem*, 61 (2008) 2968.
7 Krishna P M, Reddy K H & Pandey J P, Siddavattam D, *Transition Met Chem*, 33 (2008) 661.
8 Liu J, Lu T B, Deng H & Ji L N, *Trans Met Chem*, 28 (2003) 116.
9 Liu F Q,Wang Q X, Jiao K, Jian F F, Liu GY & Li R X, *Inorg Chim Acta*, 359 (2006) 1524.
10 Dehkordi M N & Lincoln P, *J Fluoresc*, 23 (2013) 813.
11 Jing B, Li L, Dong J, Li J & Xu T, *Transition Met Chem,* 36 (2011) 565.
12 Alaghaz A N M A, Zayed M E & Alharbi S A, *J Mol Struct*, 1082 (2015) 62.
13 Reddy P R, Rajeshwar S & Satyanarayana B, *J Photochem Photobiol B*, 160 (2016) 217.
14 Gokce C & Gup R, *Chem Pap,* 67 (2013) 1293.
15 Raman N, Jeyamurugan R, Subbulakshmi M, Boominathan R & Yuvarajan C R, *Chem Pap*, 64 (2010) 318.
16 Raman N, Sobha S & Mitu L, *Monatsh Chem,* 143 (2012) 1019.
17 Ma X F, Li D D, Tian J L, Kou Y Y & Yan S P, *Transition Met Chem*, 34 (2009) 475.
18 Kelly J M, Tossi A B, Mc Connel D J & Ohuigin C A, *Nucleic Acid Res*, 13 (1985) 6017.
19 Sakthivel A, Raman N & Mitu L, *Monatsh Chem,* 144 (2013) 605.
20 Dehkordi M N, Bordbar A K, Mehrgardi M A & Mirkhani V, *J Fluoresc*, 21 (2011) 1649.
21 Hamdi A.M, Fatin M, Ahmed N, Rashd M, Younis O, Saied M & Graham E, *Results Chem,* 5 (2023) 100775.